https://doi.org/10.5194/egusphere-2025-521
Preprint. Discussion started: 18 February 2025


# The Complex Teleconnections and Feedback Mechanisms between Mainland Indochina's Southwest Monsoon and Arctic Ocean Climate Variability

Kyaw Than Oo [1, 2]*, Aminu Dalhatu Datti[1,3], Kazora Jonah [1,4] , Brian Odhiambo Ayugi [1,5]

[1]School of Atmospheric Sciences, Nanjing University of Information Science & Technology, Nanjing, 210044, China

[2]Aviation Weather Services, Yangon, Myanmar

[3]Nigerian Meteorological Agency (NiMet), Nnamdi Azikiwe Int. Airport, Abuja-Nigeria

[4]Rwanda Meteorological Agency, Kigali, Rwanda

[5] Wyss Academy for Nature, University of Bern, Nanyuki, 10400,Kenya

*Corresponding author: kyawthanoo34@outlook.com, https://orcid.org/0000-0003-1727-3462

## Abstract

In recent decades, the Arctic climate has changed significantly, especially with a rapid decrease in Arctic Sea ice (ASI) extent in September. This study explores how natural climate variations, specifically linked to the Mainland Indochina Southwest Monsoon (MSWM), affect ASI in September using 40 years of data (1981–2020). The study found that strong MSWM years are associated with less ASI drifting to the Atlantic basin during September, leading to increased sea ice particularly in the Beaufort Sea area. Conversely, weak MSWM years tend to correspond with decreased ASI in certain locations. The MSWM influences the North Atlantic Oscillation (NAO) and North Pacific Oscillation (NPO), altering their typical patterns during strong and weak MSWM years due to interactions between monsoonal heating and the atmosphere-ocean system. During strong MSWM years, a positive NAO and negative NPO weaken the Beaufort Sea High Pressure (BSHP), whereas, during weak MSWM years, the reverse occurs, strengthening the BSHP. And the intensity of the BSHP influences Arctic air-sea interaction, influencing the movement of cold airmass and the track of the transpolar drift stream. This leads to increased sea ice formation during strong MSWM years and decreased formation during weak MSWM years in the Beaufort-Chukchi Sea region.

**Keywords:** Arctic sea ice; Mainland Indochina Southwest Monsoon; Beaufort Sea High Pressure; MSWM; North Atlantic Oscillation; North Pacific Oscillation,

https://doi.org/10.5194/egusphere-2025-521
Preprint. Discussion started: 18 February 2025


# 1 Introduction

The worldwide effects of the dramatic September thaw of Arctic Sea Ice (ASI) have recently captured the attention of both experts and the general public. Over the past fifteen years, there has been a forty percent decline in the summer area extent of ASI (Overland, 2021). According to Mueller et al., (2018) , sea ice extent minima since 2001 are lower than the historical climatological mean circumstances (1953–2012). Western Arctic seas such as the Chukchi and Beaufort saw the fastest sea ice melting of any Arctic region (Ballinger & Rogers, 2014; Perovich & Richter-Menge, 2009). There are just a few of the many observational and climate-modelling studies that point the finger at human activity for the precipitous decline in ASI (Comiso et al., 2017; Min et al., 2008; Notz & Marotzke, 2012). But new studies (Ding et al., 2019; Kay et al., 2011; J. C. Stroeve et al., 2012; Swart, 2017) imply that the climate system's internal variability influences the trend in the pan-ASI extent reduction in September. Unfortunately, we don't know what caused the sudden drop in ASI since climate models can't accurately represent the underlying natural processes (internal variability) (Deser et al., 2014). Natural climate drivers like the El Niño Southern Oscillation (ENSO), Pacific Decadal Oscillation (PDO), North Atlantic Oscillation (NAO), and Arctic Oscillation (AO) can influence the western ASI on interannual and decadal timescales through atmospheric and oceanic teleconnections (Ballinger & Rogers, 2014; L. Wang & Chen, 2014). When NAO is in its positive phase, it has been found to cause sea ice expansion in the Beaufort Sea region (Hu et al., 2002; Maslanik et al., 1996) and sea ice decline in the Siberian sector (Hurrell et al., 2003; Pinto & Raible, 2012). This is believed to be the regional expression of the AO, a large-scale hemispheric mode of variability. Sea ice extent, area, and dynamics are determined by the thermal and physical dynamics of the Arctic Ocean system, which include things like prevailing winds, ocean currents, and heat fluxes from the atmosphere and the ocean (Vihma, 2014). The wind-driven Beaufort Gyre and the Transpolar Drift are the two main features of the present Arctic Ocean that are critical for maintaining the circulation and positioning of the ASI (Spall, 2019; Timmermans & Marshall, 2020). The strength of the Beaufort Gyre is determined by a semi-permanent high-pressure system that is located above the Beaufort Sea region; this system is known as the Beaufort Sea High Pressure area (BSHP). ASI is melting at a rapid pace due in large part to the position and strength of the wind field associated with the BSHP, which can extend from the Icelandic low to the eastern Arctic (Serreze & Barrett, 2011). The ASI reached an unprecedented low in September 2007 (J. C. Stroeve et al., 2012). According to Serreze & Barrett, (2011), these shifts occurred because of the persistently negative sea level pressure (SLP) and severe BSHP anomalies that persisted throughout the

https://doi.org/10.5194/egusphere-2025-521
Preprint. Discussion started: 18 February 2025


summer over the central region of North Eurasia. Moore & Pickart, (2012) found that a strong BSHP at the beginning of summer is another indicator of polynyas in the Chukchi Sea. Fig. 1 shows that the strength of the BSHP and the related fluctuations in circulation significantly affect the variability of the ASI.

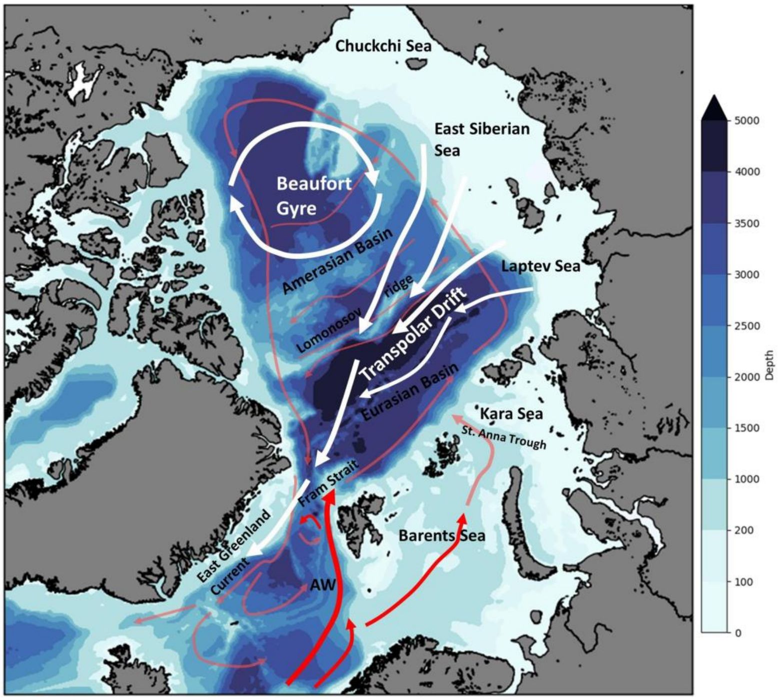


*Fig. 1 Main current features in the Arctic Ocean and North Atlantic. The coloured shaded represent the bathymetry. Atlantic water (AW, red lines) reaches the Arctic Ocean via the Fram Strait and a distinct branch across the Barents/Kara Seas, where it circulates as a subsurface current (light red). The Beaufort Gyre and Transpolar Drift are surface features (shown with white arrows) that impact sea ice drift patterns. The Lomonosov Ridge separates the Arctic Basin into the Amerasian and Eurasian basins. Pacific Water inflow is excluded* (Drivdal et al., 2021).

Understanding the complex interactions between the Asian monsoon system and ASI is essential for predicting and mitigating the effects of the current climate change. According to previous studies (Lejeune et al., 2015; Lenton et al., 2008), these components are part of a larger network of climate processes that, if disrupted, can lead to tipping points with far-reaching consequences for our climate system (Supplementary Figure S-1). Some studies have examined the connection among the ASI and monsoon, specifically the connection with the Asian monsoon. This is remarkable given that numerous studies (Clark & Lee, 2019; Cohen et al., 2014; England et al., 2019), have verified the several teleconnections between ASI and

https://doi.org/10.5194/egusphere-2025-521
Preprint. Discussion started: 18 February 2025


storm tracks, the variabilities in SST, wave trains, and the jet stream location changes. The ASI concentration and the East Asian summer monsoon are strongly correlated, according to research using observational data and climate model simulations (Chen et al., 2022; Guo et al., 2014; He et al., 2018). Similarly, an earlier study implies that the Arctic Sea ice's unpredictability impacts the Mainland Indochina Southwest Monsoon (MSWM). For instance, Sundaram & Holland, (2022) looked at the variability of sea ice in the Barents and Kara Seas during the boreal autumn and discovered that it had a significant impact on the rainfall during the south Asian summer monsoon that followed. In addition, with an emphasis on the last few years, specifically the 1980s, Chatterjee et al., (2021) also suggested a physical explanation for the connection between the seasonal sea ice range in the Kara Sea and the late-season monsoon rainfall extremes. These studies all show how the variability of ASI affects the variability of monsoons. Accordingly, a few studies showed how the monsoons in East Asia and India affect the sea ice in the Arctic. Krishnamurti et al., (2015) explained that established the link between the the ASI and Asian Monsoon during the summer. Researchers explored how the Beaufort Sea region's sea ice variability was affected by high rainfall events linked to the South Asian summer monsoon over northwest India and Pakistan. Similarly, Grunseich & Wang, (2016) show how the unique and united influences of the Indian and East Asian monsoons affect the ASI especially during summer.

It's interesting to statement that the Asian Monsoon systems and ASI have similar variability. A long-term review of MSWM rainfall by previous studies (Oo, 2022, 2023; K. K. Sein et al., 2018; Z. M. M. Sein et al., 2015), revealed a decreasing tendency over the previous few decades. Furthermore, Satyanarayana et al., (2020) showed a decrease in MSWM rainfall following the late 2000s in comparison to those years prior to 2000. The experimental studies of Aung et al., (2017) are likewise supported by these investigations.

https://doi.org/10.5194/egusphere-2025-521
Preprint. Discussion started: 18 February 2025


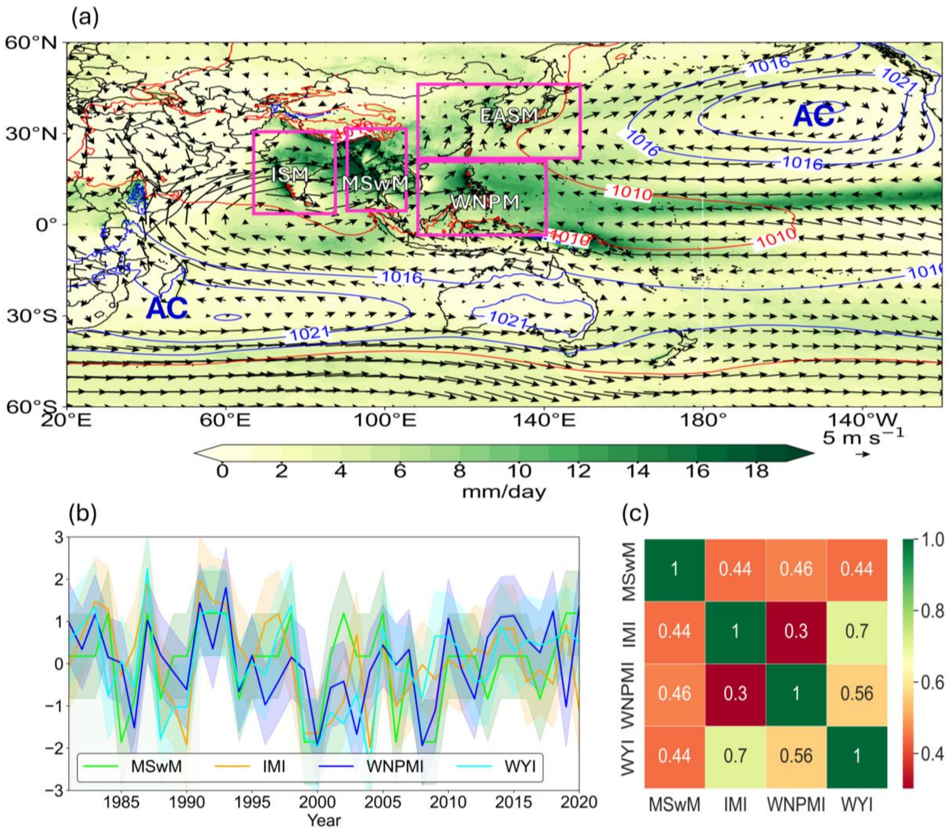


*Fig. 2 Four sub-regions of Asian-Pacific monsoon adopted from* (B. Wang & Ho, 2002). *ISM, MSWM, and WNPSM are tropical monsoon regions and the subtropical monsoon, EASM by shaded daily rainfall (mm/day) with 850 hPa level wind (vector, m/s) and geopotential (contour, gpm) during peak monsoon months(JJAS). (b) Annual time series of each monsoon indices and (c) their correlation heatmap.(Figure concept is adopted from authors previous work* (Oo et al., 2024)*)*

We were prompted to examine the possibility of a connection between MSWM and the September reduction in ASI after carefully examining all of the above-mentioned research. In our study, we examine the hypothesis that the seasonal lowest concentration month of ASI (September) is influenced by the interannual variability of the MSWM. Numerous variables, including ENSO (Webb & Magi, 2022), the Indian Ocean Dipole (Ashok et al., 2001), the amount of snow cover in Eurasia in the winter (Vernekar et al., 1995), NPO (Mantua & Hare, 2002) and NAO (Krishnamurthy & Krishnamurthy, 2016), influence the interannual fluctuation of the MSWM. In addition, it's intriguing to note that ENSO has a multi-decadal impact on Arctic sea ice, while NPO and NAO influence it scale on an interannual and predict seasonal to decadal-scale fluctuation (Flatau et al., 2003; Mantua & Hare, 2002). This research

https://doi.org/10.5194/egusphere-2025-521
Preprint. Discussion started: 18 February 2025


investigates the connection between the September ASI and the large-scale MSWM circulation by using the 40 years data record spanning between 1981 and 2020 to comprehend the effects of both weak and strong MSWM intensity on the ASI as a tropical-polar teleconnection during September.

## 2 Data and Methods

The datasets applied in our study encompass a wide range of atmospheric and oceanic variables, providing comprehensive coverage both temporally and spatially. Daily rainfall data is sourced from the APHRODITE Daily Precipitation (Yatagai et al., 2012), which offers a high-resolution and globally unified dataset critical for accurate precipitation analysis. Additional atmospheric variables are obtained from the ERA5 reanalysis (Hersbach et al., 2020), renowned for its detailed temporal (hourly) and spatial (0.25-degree grid) resolution, ensuring precise and reliable atmospheric condition insights. Wind data is derived from the NCEP reanalysis (Kalnay, 1996), another strong dataset that provides essential wind patterns and dynamics, contributing to the overall understanding of atmospheric circulation. ASI concentration is extracted from NOAA's daily gridded data, available from 1978 to the present, which is derived from satellite observations, offering invaluable insights into polar conditions with both temporal reliability and spatial precision. Moreover, the NOAA Optimum Interpolation (OI) SST V2 dataset (Reynolds et al., 2002), is the source of sea surface temperature (SST) data. This dataset combines observations from many sources to generate precise, high-resolution SST fields that are essential for oceanographic and climate research. These datasets, when combined, form a strong and complex foundation for assessing climatic and environmental changes over several decades with high spatial and temporal resolution.

In this analysis, we used common statistical methods such as standardization, anomaly computations, correlation and composite analysis, to identify the specific connection between Arctic sea-ice and MSWM variability. We performed multipart examines of ASI concentration, 925 hPa level air temperature, sea-level pressure (SLP), and conducted substantial examination tests to check the dependability structures. For computation and data manipulation, we used the Climate Data Operator, and for plotting figures and performing the statistical two-tailed test, we used Python.

### 2.1 Monsoon Intensity Index Definition

The Asian monsoon system facilitates the interhemispheric moisture flow from the southern subtropical Indian Ocean to the Indian and Indochina subcontinents, playing a critical role in regional climate dynamics. The monsoon over Indochina is shaped by four primary sub-

https://doi.org/10.5194/egusphere-2025-521
Preprint. Discussion started: 18 February 2025


monsoon systems: the Indian monsoon (ISM), mainland Indochina southwest monsoon (MSWM), east Asia summer monsoon (EASM) and the west north Pacific monsoon (Fig. 2) (Gulev et al., 2002; B. Wang & Ho, 2002). As a result, the Indochina monsoon exhibits distinct characteristics that set it apart from other regional monsoons (Oo, 2023). The region is significant for global agriculture, as about 80% of the world's rice is produced in mainland Indochina, where the MSWM is heavily influences both the intensity and seasonality of rainfall patterns (Thwe et al., 2019). Between June and September, over 65% of the region's annual rainfall occurs as a result of the MSWM (K. K. Sein et al., 2018). Moreover, our analysis also showed the significant seasonal pattern by EOF (Supplementary Figure S-2). Though the monsoon season itself is consistent, the amount of rainfall is bringing varies substantially from year to year. This variability contributes to extreme weather events, such as floods and droughts, which can disrupt both the environment and the economy of the region. The frequent occurrence of these extreme events underscores the need for a reliable index to track and predict the monsoon's behavior. Such an index would provide critical insights into the mechanisms governing the monsoon and could aid in forecasting the intensity of future monsoons, offering valuable support to operational climate centers.

In previous studies, researchers have developed various monsoon indices, with notable contributions from Goswami et al., (1999), Hung & Yanai, (2004), Lwin, (2000), B. Wang & Fan, (1999), P. J. Webster & Yang, (1992), and Yin, (1949). These indices are generally classified into two categories: upper-zonal wind shear indices and low-level wind indices. However, while useful, these indices do not fully capture the complexity of the MSWM variability. Therefore, a more specific intensity index for the MSWM is still required. Moreover, a promising approach for defining the MSWM intensity involves the use of sea level pressure (SLP) data, as suggested by several studies (Patil *et al.*, 2011; Riaz, Iqbal, and Adeel, 2021). The primary driving force behind the MSWM is the temperature contrast between the warm Asian mainland and the cooler southern hemisphere oceans (e.g. Webster, 1983). One of the first indices to quantify monsoon intensity using SLP data was the Southwest Monsoon Intensity Indicator (SMII), developed by Lwin, (2000). Compared to other meteorological variables such as near-surface winds, SLP data are more readily available and offer higher reliability (Oo et al., 2025). For these reasons, SLP-based indices have proven to be a valuable tool for both analyzing historical trends and predicting daily variations in monsoon intensity.

This study employs the SMII, which is based on the sea-level pressure (SLP) data from two key regions, Putao and Kaw Thaung, to analyse the interannual variability of the summer monsoon over the study region. The climatology of the summer mean pressure field, shown in

https://doi.org/10.5194/egusphere-2025-521
Preprint. Discussion started: 18 February 2025


Fig 2a, reveals three primary high-pressure systems and the monsoon low trough (MLT) pressure regimes. The mean standard deviation of SLP, corresponding to the climatological center of the MLT, highlights significant interannual variability. This variability, the highest in the tropical region, enhances tropical convective activity and drives wave-like teleconnections extending from the tropics to the midlatitudes (Ding *et al.*, (2011); Li, Lu, and Chen, (2017).

The correlation analysis of rainfall over the MSWM region (90°E-105°E and 10°N-30°N) with SMII show the positively dominant (Fig 3). The SMII, derived from the SLP data of the Kaw Thaung and Putao regions, is calculated as follows:

$$SMII = SLP_{KawThaung} - SLP_{Putao}$$

This index, defined as the difference in SLP between the southern Kaw Thaung station (98°E-99°E, 9°N-10°N) and the northern Putao station (98°E-99°E, 27°N-28°N), reflects local-scale pressure variations and is used to assess monsoon intensity. The normalized climatology of the SMII index, compared with the other sub-monsoon systems, displays significant correlations (Fig 2b,c).

# 3 Results and Discussions

## 3.1 Climatology point of view

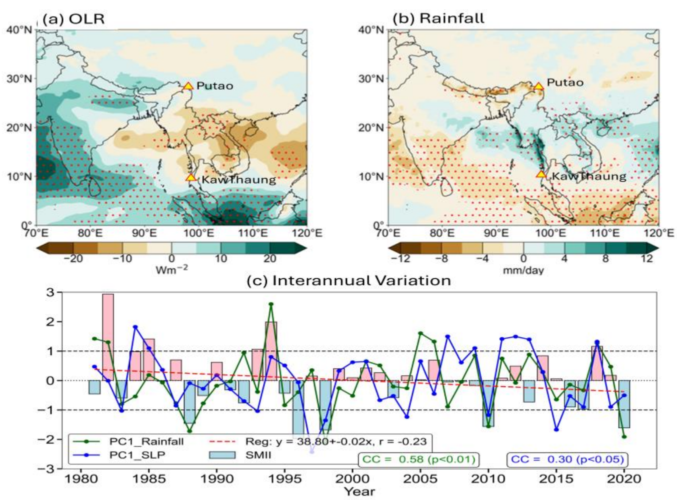


| Phase | Years | | | | |
|---|---|---|---|---|---|
| Strong | 1982 | 1985 | 1993 | 1994 | 2018 |
| Weak | 1988 | 1996 | 1998 | 2010 | 2020 |

*Fig. 3 Correlation map of (a) daily OLR and (b) daily rainfall with daily SMII. (c) Their timeseries of monsoon tensity (bar) with its trend line (red dash line)and fitst PC of slp and rainfall over maninland Indochina region with their CC values with monsoon intensity.*

https://doi.org/10.5194/egusphere-2025-521
Preprint. Discussion started: 18 February 2025


A detailed analysis of the time series reveals that the 1981–2020 period experienced five distinct years of strong monsoon (SMII > +1) {1982, 1985, 1993, 1994, and 2018} and five years of weak monsoon (SMII < -1) {1988, 1996, 1998, 2010, and 2020} (Fig. 3). According to Koteswaram (1958), one of the most significant monsoon heat sources traverses mainland Indochina during the boreal summer. A notable feature of tropical heat sources is their capacity to influence both ocean basins and landmasses remotely via teleconnections. Localized extreme rainfall, followed by a substantial release of latent heat, is often linked to deep convection and appears to be associated with these tropical heat sources (Horel, J. D., 1981; Trenberth et al., 1998).

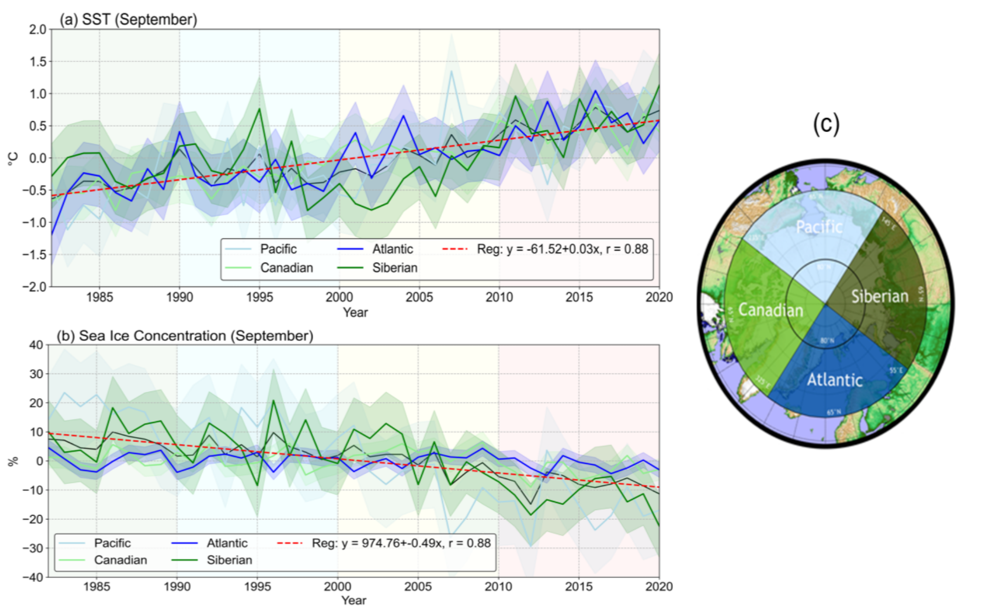


*Fig. 4 Interannual variation of (a) SST (°C) and (b) ASI concentration for four sub-region of Arctic Ocean as in (c).*

The analysis of interannual variations in Arctic sea surface temperature and ice concentration for the month of September reveals significant fluctuations, as shown in Fig. 4a. These fluctuations highlight the unpredictable nature of Arctic sea ice dynamics. Given the highly unpredictable nature of sea ice in the Arctic, a noticeable and rapid decline is evident in Fig. 4b. Previous studies, such as those by Comiso et al., 2017 and Parkinson et al., 1999, have documented that the Arctic sea ice (ASI) began its swift retreat in the late 1990s. After 1996, sea ice extent has remained consistently below the 1979-1999 average (Vihma, 2014). Walsh et al., (2017) also highlighted that the rate of ASI loss in the 1990s was unexpected, with significant reductions observed in the Chukchi and Beaufort Seas each September.

https://doi.org/10.5194/egusphere-2025-521
Preprint. Discussion started: 18 February 2025


Furthermore, statistical data show that the September sea ice extent reached record lows after 2000 (Comiso et al., 2017). Additionally, we analyze the years of weak and strong MSWM, with Figs. 5 and 6 illustrating the anomalous ASI in September, based on NOAA gridded data. Notably, out of the 21 strong MSWM years, five 1982, 1985, 1993, 1994, and 2018 show reveals lower sea ice concentration across the Laptev Sea and increasing ice over the Beaufort Sea, as indicated in Fig. 5. Conversely, among the 19 weak monsoon years, five exhibit a significant reverse pattern, as shown in Fig. 6. However, some strong and weak monsoon years present deviations from these typical patterns, likely influenced by other atmospheric factors. Identifying the causes of these anomalies will be an important focus for future research.

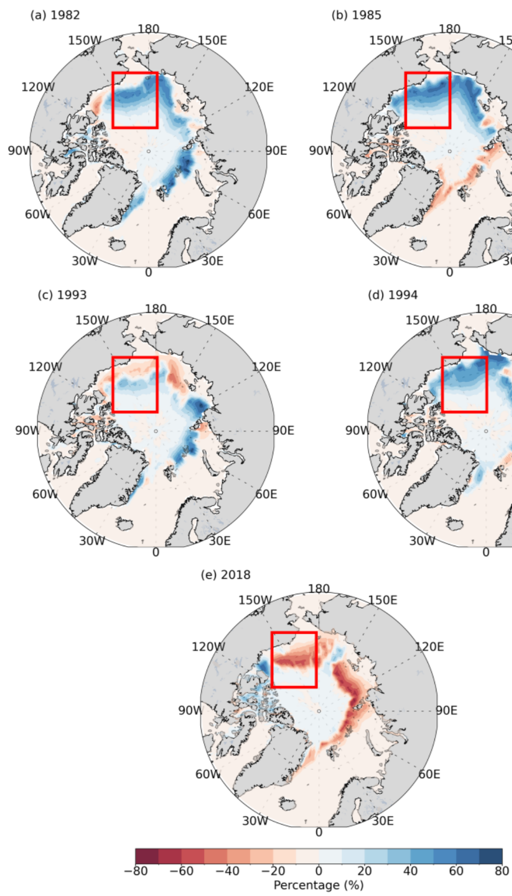


*Fig. 5 Anomalies of ASI concentration percentage over Arctic region during September of strong MSWM years during 1981–2020.*

https://doi.org/10.5194/egusphere-2025-521
Preprint. Discussion started: 18 February 2025


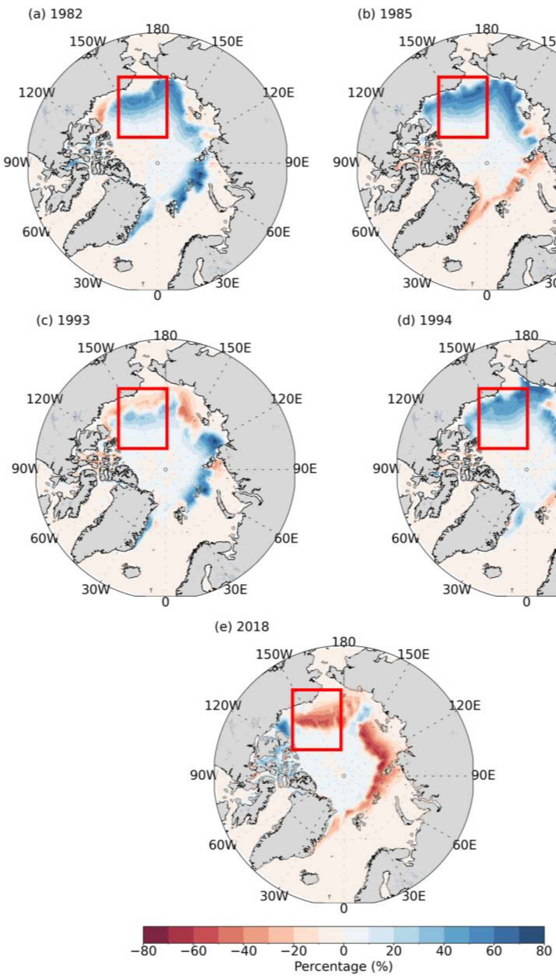


*Fig. 6 Anomalies of ASI concentration percentage over Arctic region during September of weak MSWM years during 1981–2020.*

To validate the characteristics of anomalous Arctic sea ice (ASI) concentration, we conducted climatological composite analyses for both strong and weak MSWM years (Fig. 7a,b). Additionally, we computed the difference between these two phases to facilitate comparison (Fig. 7c). Assessing statistical significance required the assumption that the sample means of both phases originated from the same population specifically, the anomalous ASI concentration during strong and weak MSWM years. To ensure strength, we selected five years with the strong intense and weak intense MSWM events for analysis. The results confirmed statistically significant estimates.

https://doi.org/10.5194/egusphere-2025-521
Preprint. Discussion started: 18 February 2025


Further computations followed the same methodology, with the 95% confident dotted regions in Fig. 7c highlighting areas where the ASI anomalies over the Beaufort Sea are both pronounced and statistically significant. Our analysis exposes that ASI concentration in the Beaufort Sea increases during strong MSWM years but declines during weak MSWM years. Interestingly, the opposite pattern emerges in the eastern Arctic, particularly over the Laptev and Kara Seas. To highlight these findings, we conducted a complementary composite analysis using the gridded HadISST sea ice and SST dataset. The results (Supplementary Materials, Figure S-3) also strongly verify our initial observations. In particular, our study suggests that strong MSWM years are generally linked to reduced sea ice extent in the eastern Arctic but increased ice cover in the northwestern Arctic (Fig. 7c), whereas weak MSWM years exhibit the reverse pattern.

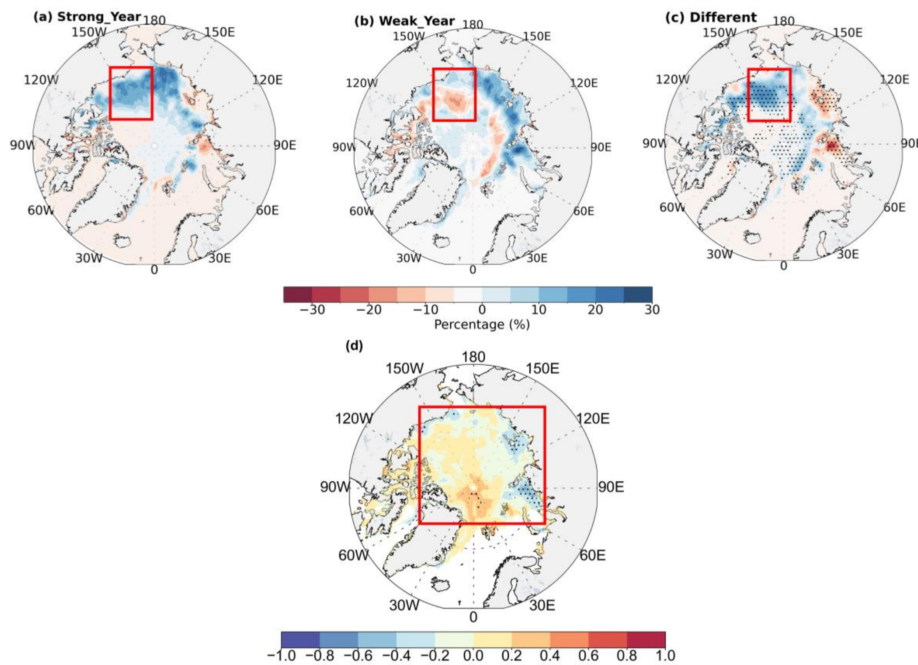


*Fig. 7 The mean of Composites anomalous ASI concentration for (a) MSWM strong intensity years (b) MSWM weak intensity years, (c) their difference in percentage (strong minus weak) and (d) correlation values with SMII with 95% confidence level dotted.*

In summary, this study investigates the variability of summer Pacific SST driven by ENSO but does not account for other atmosphere-ocean interactions that may influence the MSWM. The inverse relationship between El Niño and MSWM is well documented (Zaw et al., 2020; Zin Mie Mie Sein et al., 2015). Our analysis reveals that every strong MSWM year, including

https://doi.org/10.5194/egusphere-2025-521
Preprint. Discussion started: 18 February 2025


1985, coincided with a La Niña event (Fig. 3c, Fig. 5). Additionally, climatological analyses show that sea ice in the Arctic's Beaufort Sea expands during strong MSWM years and diminishes during weak ones. These findings prompted us to explore whether interannual MSWM variations significantly impact sea ice variability, particularly in the Beaufort Sea region. To confirm this, we have to analysis more detailed regarding air-sea interaction over global general circulation.

## 3.2 MSWM–NAO-NPO-Arctic Sea-Ice Teleconnections and Interactions

Natural fluctuations in low atmospheric pressure are a major cause of climate variability (B. Wang et al., 2005; P. Webster, 2020). We investigated the sea level pressure anomaly and upper wind (200 hPa) composites of strong/weak MSWM years to comprehend and begin the connection among MSWM and ASI concentration in the Arctic throughout the summer.

During strong MSWM years (Fig. 8a), there is unusually high sea level pressure from the Sahara-Mediterranean section to the far north Atlantic. This includes specific high-pressure areas over the Azores, the high-pressure system over North Pacific subtropical regions, Eastern Eurasia, and the British Isles-Scandinavian region (C. Wang, 2002). The northern Pacific high pressure system region findings by Nigam & Baxter, (2015) and Yadav, (2009), and researcher exhibited that the subtropical high over the North Pacific during summer time of northern hemisphere is a Kelvin wave feedback to heat from the MSWM, while the negative pressure anomalies appear in the Iceland-Greenland region. These unusual high and low-pressure patterns over the Atlantic area are typical of the positive-phase of the NAO during summer (Corti & Palmer, 1997). In the Arctic, there is a reduction of sea level pressure, with clear low-pressure anomalies in the Beaufort Sea and some parts of central North Eurasia. Interestingly, strong MSWM years show low pressure over the Bay of Bengal and Mainland Indochina region (Fig. 8a exhibit features), which is opposite to what is observed during weak MSWM phases. Through weak MSWM (Fig. 8b), the whole Arctic Sea level pressure increases, with high-pressure centers forming over the Greenland and Beaufort Sea, while low pressure areas appear over the British Isles-Scandinavian, Sahara-Mediterranean, Azores, and North Pacific subtropical regions. All these low and high-pressure zones are statistically significant (Fig. 8c). Therefore, Fig. 8 shows that the positive NAO occurs during strong MSWM years, and the negative NAO occurs during weak MSWM years.

https://doi.org/10.5194/egusphere-2025-521
Preprint. Discussion started: 18 February 2025


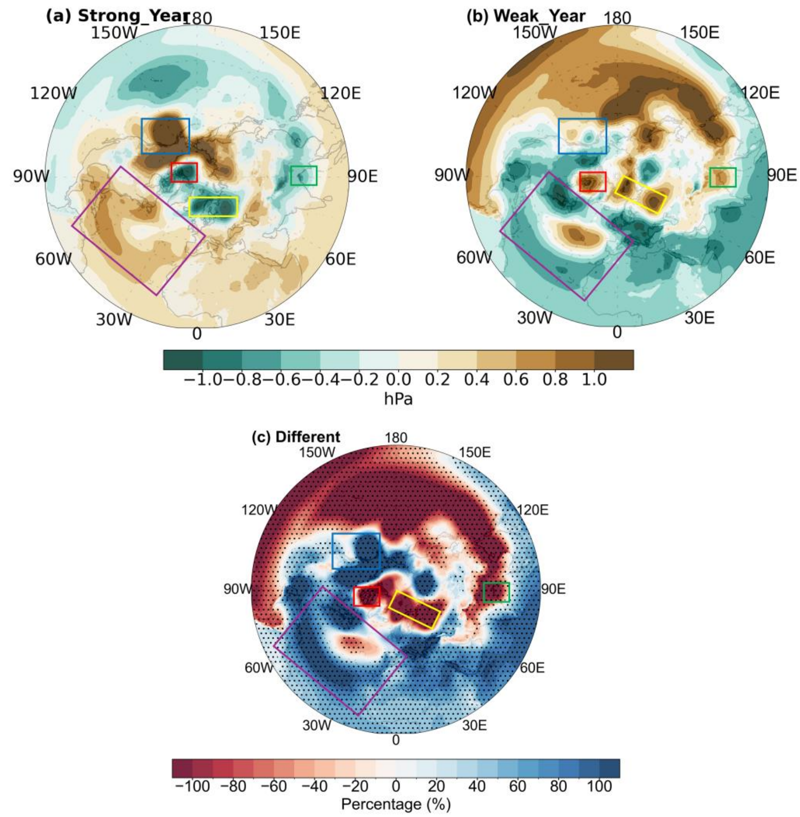


*Fig. 8 Composites (June–September) SLP (hPa) anomaly, with 90% confidence dotted area, (a) MSWM strong intensity, (b) MSWM weak intensity, and (c) their difference in percentage (strong minus weak). The main regions of North America, Europe, and Africa were represented by a rectangle box: the North Atlantic (purple), North Pacific (blue), Beaufort Sea and North Eurasia (red), Greenland-Iceland (yellow), and mainland Indochina (green).*

Similarly in the North Pacific Ocean, close to the Aleutian Islands, lies a semi-permanent low-pressure system termed the Aleutian Low (Collins et al., 2006; Xue & He, 2007). It plays an important role in the North Pacific weather patterns. The strength and position of the Aleutian Low are intimately tied to the North Pacific Oscillation (NPO), which affects weather patterns in the North Pacific and has downstream consequences on North America. NPO is a prominent atmospheric variability pattern in the North Pacific region, characterized by fluctuations in sea-level pressure. The negative stage of the NPO has significant teleconnections with various climate systems, including the Asian monsoon, ENSO (El Niño-Southern Oscillation), the Aleutian low-pressure system, and the North Pacific high-pressure system (Fig. 8a). The negative NPO tends to weaken the subtropical high-pressure system over

https://doi.org/10.5194/egusphere-2025-521
Preprint. Discussion started: 18 February 2025


the north-western Pacific, which in turn affects the monsoon circulation. During the NPO negative phase, the reduced subtropical high can lead to a stronger and more northerly displaced summer monsoon in the MSWM region including the east Asian monsoon region, bringing more precipitation to the region (Ha et al., 2012). Conversely, the Indian monsoon might experience a weakening due to the altered pressure gradients and wind patterns (Fig. 8).

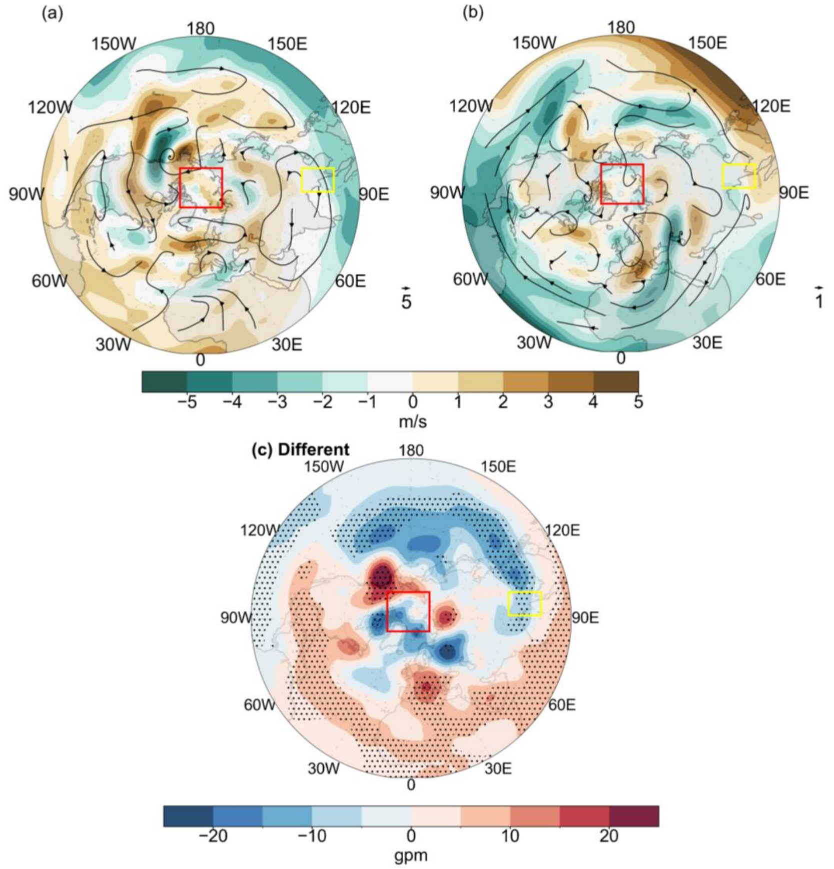


*Fig. 9 Composites of June–September (JJAS) 200 hPa geopotential (gpm) anomaly (a) MSWM strong intensity, (b) MSWM weak intensity, and (c) their difference in percentage (strong minus weak) with dotted 90% significance level.*

To verify the importance of these patterns, we compared the unusual upper air circulation pattern (shown in Fig. 9) to the years with strong and weak MSWM. All major significant regions show a similar pattern of positive and negative anomalies, as shown in Fig. 8. There is a positive link with a negative correlation in the eastern region between the rainfall over the mainland Indochina region and the ASI concentration over Arctic seas (Fig 7d). The pattern showed similarities to the composite analysis shown in Fig. 7c.

https://doi.org/10.5194/egusphere-2025-521
Preprint. Discussion started: 18 February 2025


Homogeneous sea level pressure (SLP) anomalies, there are significant positive and negative correlations between rainfall over specific regions. Positive correlations occur across the North Pacific high-pressure and the Azores regions, while negative correlations are found in the Beaufort Sea and Greenland-Iceland region. These correlation and sea-level pressure studies suggest that the MSWM influences Arctic atmospheric circulation from a distance. The NAO  (Qu et al., 2012; Yadav et al., 2009) and NPO  (Nigam & Baxter, 2015b) are important in this teleconnection, however, their variability is not yet fully understood. According to Bian et al., (2018), NAO anomalies are created by the breaking of upper-level Rossby waves on a synoptic scale. The positive phase is caused by anticyclonic breaking, and the negative phase is caused by cyclonic breaking. This makes one wonder if the phase of the NAO is impacted by the MSWM.

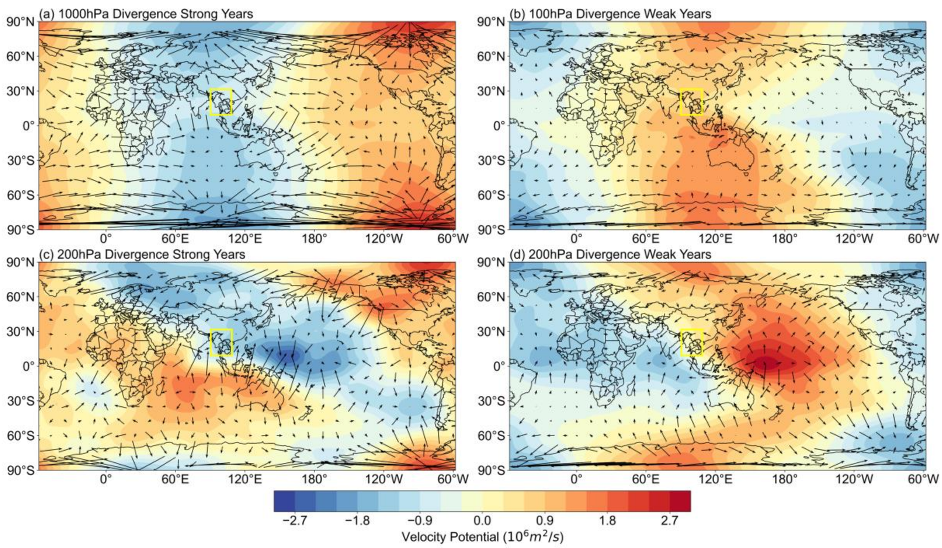


*Fig. 10 JJAS anomalous divergent wind (vectors, ms$^{-1}$)and Velocity potential (1 × 10$^{6}$ m$^{2}$ s$^{-1}$, shading) for MSWM strong intensity years (left column, (a,b) and MSWM weak intensity years (right column, (c,d)) MSWM years of 200hPa and 1000hPa level. The MSWM region was represented by a yellow rectangle box.*

To understand the connection of MSWM with NPO and NAO, we analyzed the lower and upper atmospheric velocity potential (a stand-in for the Walker cell circulation), and wind divergences (Fig. 10). The solid MSWM composite shown in Fig. 10 explained the convergence at the lower atmospheric layer (1000hPa level) over the southwest monsoon region, predominantly monsoon trough area, due to the large-scale convection and heating induced by MSWM. At the same time, a divergence of anomalies is expanding from the Azores and the North Atlantic high-pressure area to the northeast Pacific Aleutian areas, as well as

https://doi.org/10.5194/egusphere-2025-521
Preprint. Discussion started: 18 February 2025


from the Eastern Sahara-Mediterranean area. This wind divergence corresponds with the high-pressure regions shown by the velocity potential in Fig. 8a.

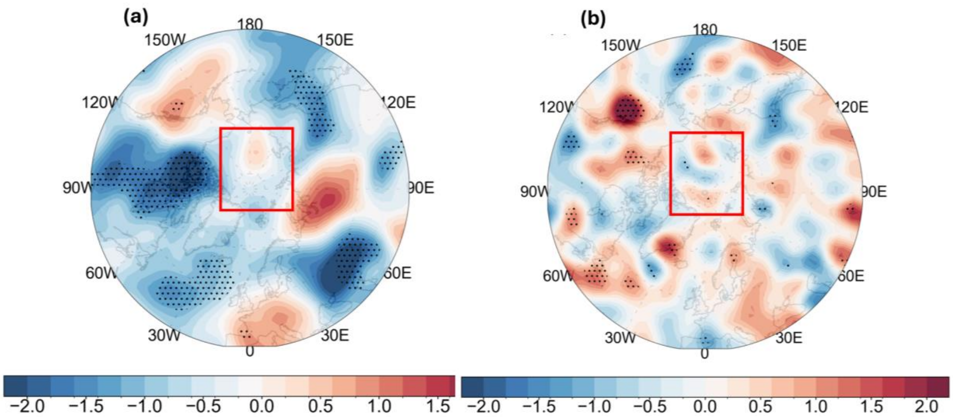


*Fig. 11 Composites of (a) June-September temperature (°C) anomalies at lower atmospheric (925 hPa) difference between strong and weak MSWM, and (b) similar as (a) but for 500 hPa vertical velocity (hpa) with dotted 95% significance level.*

Similarly, at the upper atmospheric layer (200 hPa), we observe opposite patterns: strong divergence around the MSWM regions (Fig. 10b) and convergence above the Azores/North Atlantic, Sahara-Mediterranean, and northeast Pacific high pressure regions. These circulation patterns highlight the important role of the MSWM in increasing divergence over the high pressure of subtropical Atlantic due to monsoon-induced convective caused by monsoon-forced adiabatic processes. This process suggests that the heating connected to the MSWM triggers Rossby waves concerning the westward, which interact with westerlies over mid-latitude, leading to the strong and high pressure sinking over the Atlantic subtropical high and Eastern Sahara-Mediterranean regions (Rodwell & Hoskins, 1996). The intensity of the monsoon also impacts the intensity of this descent (Shaw, 2014). The negative area of velocity potential, indicating the lower-level (1000hPa) divergence, enlarges from the Sahara-Mediterranean area to the far northern Atlantic, and matches the characteristics of the negative NAO. In years with weak MSWM, the lower (Fig. 10c) and upper (Fig. 10d) levels show opposite characteristics compared to strong MSWM years. Therefore, the intensity variability of the MSWM during southwest monsoon season (JJAS) influences the magnitude of NAO during southwest summer monsoon season, resulting in the negative (positive) phase of NAO during weak (strong) MSWM years. As shown in Fig. 11a, the impact of SLP fluctuation can

https://doi.org/10.5194/egusphere-2025-521
Preprint. Discussion started: 18 February 2025


be seen in the lower troposphere Arctic temperatures. The differences in lower atmospheric layer (925 hPa) temperature and mid-level (500 hPa) vertical velocity anomalies between strong and weak MSWM years are presented in Fig. 11a and,b respectively, with significant (95% confident) regions marked with dots.When the MSWM is strong, the Beaufort Sea region experiences significant cooling, while the Laptev Sea and Kara Sea region experiences unusual warming. The cooling happens because the weakened BSHP reduces the regional temperature and contributes to sea-ice growth. When the MSWM is weak, the opposite occurs, with warming in the Beaufort-Chukchi Sea region. This warming is due to a strong BSHP, which brings warm air and causes sea-ice to melt, as seen during the notable ASI melt in 2007 (Ballinger & Rogers, 2014; J. Stroeve et al., 2008).

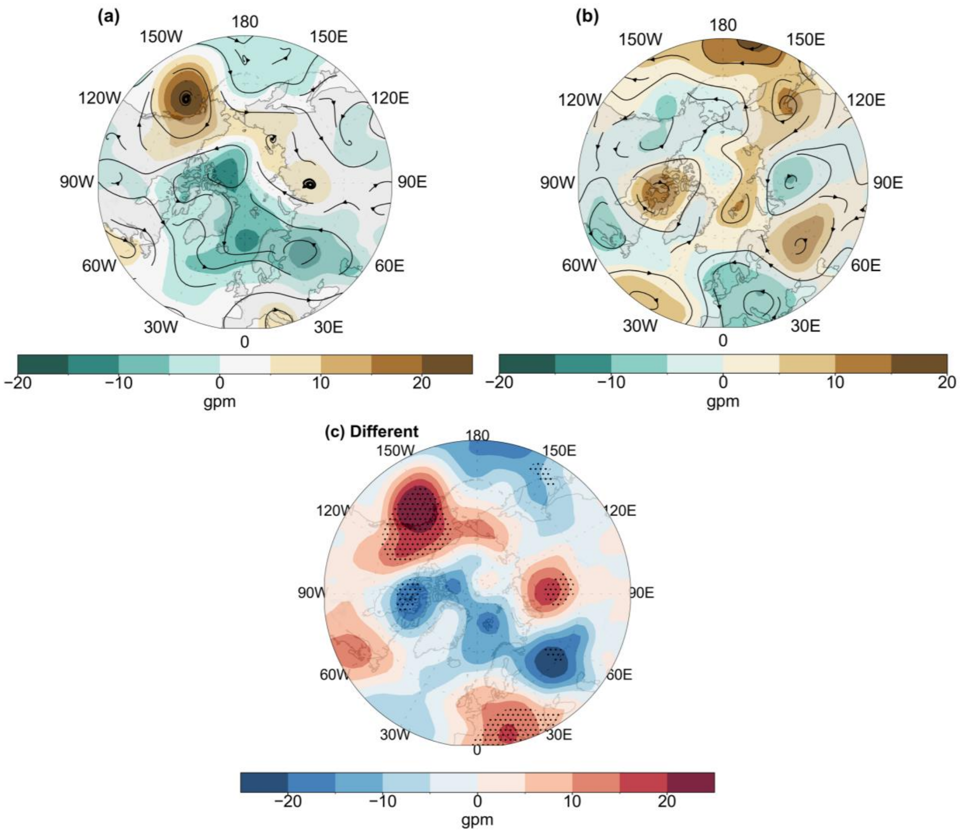


*Fig. 12 Composites of June-September anomalous 850 hPa level geopotential height (shaded, m) and streamlines (a) MSWM strong intensity, (b) MSWM weak intensity, and (c) their difference in percentage (strong minus weak) with dotted 90% significance level.*

https://doi.org/10.5194/egusphere-2025-521
Preprint. Discussion started: 18 February 2025


The next step is to look at the North Atlantic and Pacific MSWM-induced air circulation variations and see how this influence the Arctic atmospheric condition and sea-ice circulation by wind-induced. We investigate the abnormal low-level geopotential height (850 hPa) and streamlines (Fig. 12). In years with substantial MSWM, and circulation anomalies (Fig. 12a) show the weak phase of BSHP and a high pressure over Siberia. While the NAO has turned to a positive phase, the weakening of BSHP is a regular occurrence (Kwok, 2000), and it is also shown in Fig. 7a. In the Arctic, differences in air pressure create varying wind patterns. Higher pressure in the northeastern parts of the Arctic and lower pressure in the south-western parts of Arctic cause abnormal winds. These winds push sea ice counterclockwise in the eastern area of Arctic. ASI is transported from the eastern Arctic Laptev Sea to the north-western Chukchi-Beaufort Sea via the Transpolar Drift and eventually crosses out the Fram Strait. Strong Meridional Surface Wind Anomalies (MSWM) in certain years lead to colder temperatures (Fig. 11a), and the exceeding of ASI concentration in the Beaufort Sea region due to unusual wind patterns (Fig. 12a).

In contrast, during years with weak MSWM (Fig. 12b), the direction of air circulation over the Arctic changes by the negative NAO phase and the stronger BSHP. Thus, Sea ice flows directly into the Fram Strait in this scenario due to the pressure differential between the low-pressure system over the BSHP, which results in a reduction in ASI concentration in the Beaufort Seas. This analysis indicates that MSWM-induced North Atlantic air circulation significantly influences the northern hemisphere summer Arctic, sea-ice drift, ASI concentration and atmospheric circulation.

## 4 Conclusions

The primary focus of this research is the role that atmospheric teleconnections play as a natural climatic driver on Earth, connecting the polar regions with the tropics. Understanding the teleconnection between MSWM intensity fluctuation and September ASI variability, especially in the Beaufort Sea regions, is the primary goal of the study. Over the course of four decades, from 1981 to 2020, we examine datasets culled from a variety of sources, including the ERA5 reanalysis, the APHRODITE precipitation dataset, the monthly gridded data collection for Sea Ice from NOAA, and HadISST. According to the results, the MSWM affects the amounts of sea ice in the Kara Sea, the Beaufort Sea, and the Laptev Sea. The study provides a scientific basis for understanding the impact of the MSWM's yearly variations on Arctic Sea ice.

https://doi.org/10.5194/egusphere-2025-521
Preprint. Discussion started: 18 February 2025


During years with strong (weak) MSWM, the monsoon-driven adiabatic processes, influenced by diabatic heating related to MSWM, impact the summer NAO. During periods of strong (weak) MSWM intensity, the pressure changes between the Sahara-Mediterranean region and the northern subtropical Atlantic increase (decrease). This alters the summer pattern of the North Pacific Oscillation (NPO), resulting in decreased (increased) pressure over the subtropical Pacific. Hence, the positive (negative) stage of NAO and the negative (positive) stage of the NPO weaken (strengthen) the BSHP. Because of these shifts, the Arctic's sea ice and atmospheric rotation are changing, which means that the Beaufort Sea region will see exceed sea ice than usual. The enhancement (reduction) in sea ice is partially due to colder (warmer) air temperatures and anomalous cyclonic (anticyclonic) wind patterns in the area (Fig. 13). This study demonstrates the significant impact of MSWM on the summer Arctic climate, establishing a new connection between tropical and Arctic climates.

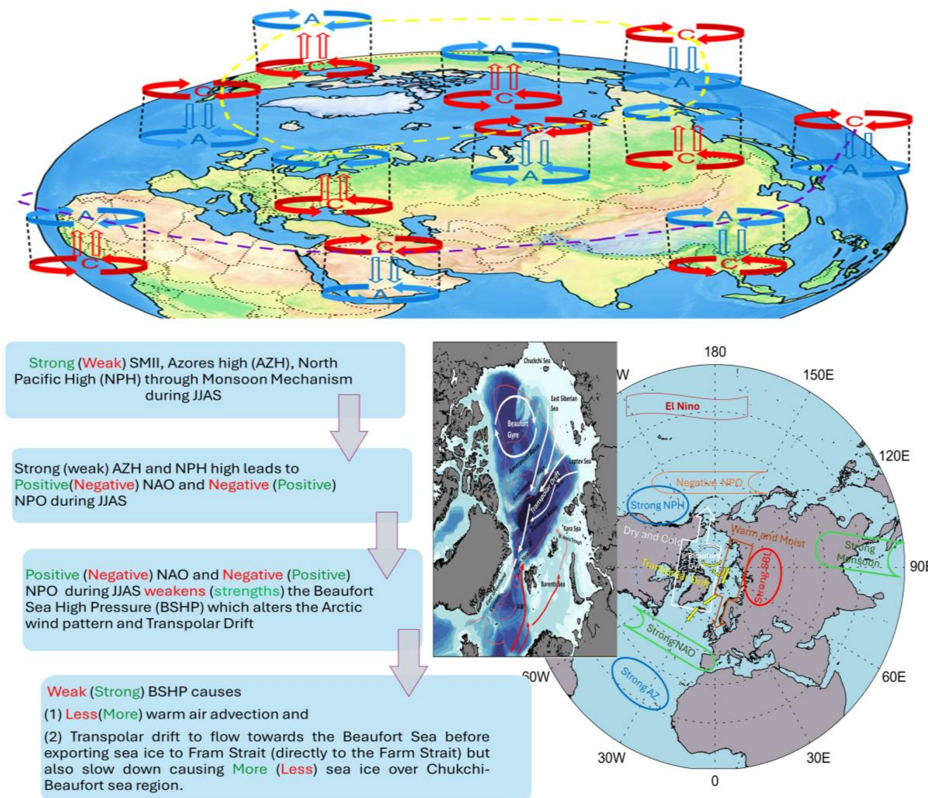


*Fig. 13 Schematic illustrative of the physical mechanismMSWM demonstrating how the MSWM and the ASI are teleconnected.*

https://doi.org/10.5194/egusphere-2025-521
Preprint. Discussion started: 18 February 2025


This finding examines the annual variations in ASI from 1981 to 2020, focusing on their correlation with the intensity fluctuations of the MSWM. The intensity of the MSWM significantly influenced the annual variation of September ASI throughout the study period. Our analysis indicates that the deterioration of the MSWM and heightened severe rainfall in northern Indochina and Southwestern China after 2005 may have played a role in the swift reduction of ASI post-2000. Nevertheless, additional study employing climate model simulations is necessary to validate this concept. Future research will examine the timeframe from 2001 to the present to evaluate this theory, ascertain whether MSWM can forecast changes in ASI, investigate the reasons behind the weakening of MSWM and the North Atlantic Oscillation (NAO), and comprehend the associated feedback mechanisms.

https://doi.org/10.5194/egusphere-2025-521
Preprint. Discussion started: 18 February 2025


## Data Availability

All data and software are open sources for anyone particularly ocean data can be accessible from NOAA Optimum Interpolation (OI) SST V2 and data can be downloaded from https://psl.noaa.gov/data/gridded/data.noaa.oisst.v2.html. In addition, the other atmospheric variable of ERA5 reanalysis data can be accessed from https://cds.climate.copernicus.eu/ . The daily rainfall data can be accessed from Aphrodite's daily rainfall https://www.chikyu.ac.jp/precip/english/ . For monthly plotting and calculation of each figure, the coding is performed by using Climate Data Operators, OpenGrADS, and Python. These can also be made available upon request by emailing to kyawthanoo34@outlook.com.

## Conflicts of Interest

I declared that there is no potential conflict of interest with any of the following statements.

1. For any component of the submitted work, the author received no cash or services from a third party (government, commercial, private foundation, etc). (including but not limited to grants, data monitoring board, study design, manuscript preparation, statistical analysis, etc.).
2. The author is not affiliated with any entity that has a direct or indirect financial interest in the manuscript's subject matter.
3. The author was involved in the following aspects of the project: (a) idea and design, or data analysis and interpretation; (b) authoring the article or critically reviewing it for essential intellectual content; and (c) approval of the final version.
4. This work has not been submitted to and is not currently being reviewed by, any other journal or publishing venue.
5. The author has no patents that are broadly relevant to the work, whether proposed, pending, or issued.
6. The author received no payment or services from a third party for any aspect of the submitted work (government, commercial, private foundation, etc). (including but not limited to grants, data monitoring board, study design, manuscript preparation, statistical analysis, etc.).

## Funding Statement

This research and publishing are being carried out using self-funding.

https://doi.org/10.5194/egusphere-2025-521
Preprint. Discussion started: 18 February 2025


## Author Contribution

Kyaw Than Oo - Conceptualization, formal analysis, methodology, analysis, visualization of data and results, the writing of the manuscript, and the drafting of the article.

Brian Odhiambo Ayugi , Kazora Jonah and Aminu Dalhatu Datti - Writing – review & editing

## Acknowledgments

The author acknowledges heartfelt thanks to the scientists of the ECMFW for supporting ERA5 datasets. The Department of Meteorology and Hydrology, Myanmar (DMH) is also acknowledged for providing the observed rainfall datasets. Also, thanks to the Nanjing University of Information Science and Technology (NUIST) for supporting my skills and techniques. In addition, show deep gratitude to Professor Haishan CHEN from NUIST, who supervises my PhD study, and supported the basic methods and concepts for this study. Furthermore, authors show gratitude Dr Suchithra Sundaram from Centre for Global Sea Level Change, New York University Abu Dhabi for the support of basic concept of this study.

https://doi.org/10.5194/egusphere-2025-521
Preprint. Discussion started: 18 February 2025


## References

Ashok, K., Guan, Z., & Yamagata, T. (2001). Impact of the Indian Ocean dipole on the relationship between the Indian monsoon rainfall and ENSO. *Geophysical Research Letters*, *28*(23), 4499–4502. https://doi.org/10.1029/2001GL013294

Aung, L. L., Zin, E. E., Theingi, P., Elvera, N., Aung, P. P., Han, T. T., Oo, Y., & Skaland, R. G. (2017). Myanmar Climate Report. *Norwgian Meterological Institute*, *9*, 105.

Ballinger, T. J., & Rogers, J. C. (2014). Climatic and atmospheric teleconnection indices and western Arctic sea ice variability. *Physical Geography*, *35*(6), 459–477. https://doi.org/10.1080/02723646.2014.949338

Bian, J., Fang, J., Chen, G., & Liu, C. (2018). Circulation Features Associated with the Record-breaking Typhoon Silence in August 2014. *Advances in Atmospheric Sciences*, *35*(10), 1321–1336. https://doi.org/10.1007/S00376-018-7294-4

Chatterjee, S., Ravichandran, M., Murukesh, N., Raj, R. P., & Johannessen, O. M. (2021). A possible relation between Arctic sea ice and late season Indian Summer Monsoon Rainfall extremes. *Npj Climate and Atmospheric Science*, *4*(1). https://doi.org/10.1038/S41612-021-00191-W

Chen, D., Gao, Y., Zhang, Y., & Wang, T. (2022). Effects of spring Arctic sea ice on summer drought in the middle and high latitudes of Asia. *Atmospheric and Oceanic Science Letters*, *15*(3). https://doi.org/10.1016/J.AOSL.2021.100138

Clark, J. P., & Lee, S. (2019). The Role of the Tropically Excited Arctic Warming Mechanism on the Warm Arctic Cold Continent Surface Air Temperature Trend Pattern. *Geophysical Research Letters*, *46*(14), 8490–8499. https://doi.org/10.1029/2019GL082714

Cohen, J., Screen, J. A., Furtado, J. C., Barlow, M., Whittleston, D., Coumou, D., Francis, J., Dethloff, K., Entekhabi, D., Overland, J., & Jones, J. (2014). Recent Arctic amplification and extreme mid-latitude weather. *Nature Geoscience*, *7*(9), 627–637. https://doi.org/10.1038/ngeo2234

Collins, W. D., Rasch, P. J., Boville, B. A., Hack, J. J., McCaa, J. R., Williamson, D. L., Briegleb, B. P., Bitz, C. M., Lin, S. J., & Zhang, M. (2006). The formulation and atmospheric simulation of the Community Atmosphere Model version 3 (CAM3). *J Clim*, *19*(11), 2144–2161. https://doi.org/10.1175/jcli3760.1

Comiso, J. C., Meier, W. N., & Gersten, R. (2017). Variability and trends in the Arctic Sea ice cover: Results from different techniques. *Journal of Geophysical Research: Oceans*, *122*(8), 6883–6900. https://doi.org/10.1002/2017JC012768

Corti, S., & Palmer, T. N. (1997). Sensitivity analysis of atmospheric low-frequency

https://doi.org/10.5194/egusphere-2025-521
Preprint. Discussion started: 18 February 2025


variability. *Q. J. R. Meteorol. Soc.*, *123*(544), 2425–2447. https://doi.org/10.1002/qj.49712354413

Deser, C., Phillips, A. S., Alexander, M. A., & Smoliak, B. V. (2014). Projecting North American climate over the next 50 years: Uncertainty due to internal variability. *Journal of Climate*, *27*(6), 2271–2296. https://doi.org/10.1175/JCLI-D-13-00451.1

Ding, Q., Schweiger, A., L'Heureux, M., Steig, E. J., Battisti, D. S., Johnson, N. C., Blanchard-Wrigglesworth, E., Po-Chedley, S., Zhang, Q., Harnos, K., Bushuk, M., Markle, B., & Baxter, I. (2019). Fingerprints of internal drivers of Arctic sea ice loss in observations and model simulations. *Nature Geoscience*, *12*(1), 28–33. https://doi.org/10.1038/S41561-018-0256-8

Ding, Q., Wang, B., Wallace, J. M., & Branstator, G. (2011). Tropical-extratropical teleconnections in boreal summer: Observed interannual variability. *Journal of Climate*, *24*(7), 1878–1896. https://doi.org/10.1175/2011JCLI3621.1

Drivdal, M., Kunisch, E. H., Bluhm, B. A., Gradinger, R., Falk-Petersen, S., & Berge, J. (2021). Connections to the Deep: Deep Vertical Migrations, an Important Part of the Life Cycle of Apherusa glacialis, an Arctic Ice-Associated Amphipod. *Frontiers in Marine Science*, *8*(December), 1–14. https://doi.org/10.3389/fmars.2021.772766

England, M., Jahn, A., & Polvani, L. (2019). Nonuniform contribution of internal variability to recent Arctic sea ice loss. *Journal of Climate*, *32*(13), 4039–4053. https://doi.org/10.1175/JCLI-D-18-0864.1

Flatau, M. K., Talley, L., & Niiler, P. P. (2003). The North Atlantic Oscillation, surface current velocities, and SST changes in the subpolar North Atlantic. *Journal of Climate*, *16*(14), 2355–2369. https://doi.org/10.1175/2787.1

Goswami, B. N., Krishnamurthy, V., & Annmalai, H. (1999). A broad-scale circulation index for the interannual variability of the Indian summer monsoon. *Quarterly Journal of the Royal Meteorological Society*, *125*(554), 611–633. https://doi.org/10.1002/qj.49712555412

Grunseich, G., & Wang, B. (2016). Arctic sea ice patterns driven by the asian summer monsoon. *Journal of Climate*, *29*(24), 9097–9112. https://doi.org/10.1175/JCLI-D-16-0207.1

Gulev, S., Jung, T., & Ruprecht, E. (2002). Climatology and interannual variabilities in the intensity of synoptic-scale processes in the North Atlantic from the NCEP/NCAR Re-analysis data. *Journal of Climate*, *15*, 809–828. https://doi.org/10.1175/1520-0442(2002)015

Guo, D., Gao, Y., Bethke, I., Gong, D., Johannessen, O. M., & Wang, H. (2014). Mechanism on how the spring Arctic sea ice impacts the East Asian summer monsoon. *Theoretical and Applied Climatology*, *115*(1–2), 107–119. https://doi.org/10.1007/S00704-013-0872-6

Ha, K. J., Heo, K. Y., Lee, S. S., Yun, K. S., & Jhun, J. G. (2012). Variability in the East Asian Monsoon: A review. *Meteorological Applications*, *19*(2), 200–215. https://doi.org/10.1002/met.1320

He, S., Gao, Y., Furevik, T., Wang, H., & Li, F. (2018). Teleconnection between sea ice in the Barents Sea in June and the Silk Road, Pacific–Japan and East Asian rainfall patterns in August. *Advances in Atmospheric Sciences*, *35*(1), 52–64. https://doi.org/10.1007/S00376-017-7029-Y

Hersbach, H., Bell, B., Berrisford, P., Hirahara, S., Horányi, A., Muñoz-Sabater, J., Nicolas, J., Peubey, C., Radu, R., Schepers, D., Simmons, A., Soci, C., Abdalla, S., Abellan, X., Balsamo, G., Bechtold, P., Biavati, G., Bidlot, J., Bonavita, M., … Thépaut, J. N. (2020). The ERA5 global reanalysis. *Quarterly Journal of the Royal Meteorological Society*, *146*(730), 1999–2049. https://doi.org/10.1002/QJ.3803

Horel, J. D., and J. M. W. (1981). *Planetary-scale atmospheric phenomena associated with the interannual variability of sea surface temperature in the equatorial Pacific*.

Hu, A., Rooth, C., Bleck, R., & Deser, C. (2002). NAO influence on sea ice extent in the Eurasian coastal region. *Geophysical Research Letters*, *29*(22). https://doi.org/10.1029/2001GL014293

Hung, C. W., & Yanai, M. (2004). Factors contributing to the onset of the Australian summer monsoon. *Quarterly Journal of the Royal Meteorological Society*, *130*(597 PART B), 739–758. https://doi.org/10.1256/qj.02.191

Hurrell, J. W., Kushnir, Y., Ottersen, G., & Visbeck, M. (2003). An overview of the north atlantic oscillation. *Geophysical Monograph Series*, *134*, 1–35. https://doi.org/10.1029/134GM01

Kalnay, E. (1996). The NCEP/NCAR 40-Year Reanalysis Project. *Bull. Amer. Meteor. Soc.*, *77*, 437–471. https://doi.org/10.1175/1520-0477(1996)077<0437:tnyrp>2.0.co

Kay, J. E., Holland, M. M., & Jahn, A. (2011). Inter-annual to multi-decadal Arctic sea ice extent trends in a warming world. *Geophysical Research Letters*, *38*(15). https://doi.org/10.1029/2011GL048008

Koteswaram, P. (1958). The Easterly Jet Stream in the Tropics. *Tellus*, *10*(1), 43–57. https://doi.org/10.3402/tellusa.v10i1.9220

https://doi.org/10.5194/egusphere-2025-521
Preprint. Discussion started: 18 February 2025


Krishnamurthy, L., & Krishnamurthy, V. (2016). Teleconnections of Indian monsoon rainfall with AMO and Atlantic tripole. *Climate Dynamics*, *46*(7–8), 2269–2285. https://doi.org/10.1007/S00382-015-2701-3

Krishnamurti, T. N., Krishnamurti, R., Das, S., Kumar, V., Jayakumar, A., & Simon, A. (2015). A pathway connecting the monsoonal heating to the rapid Arctic ice melt. *Journal of the Atmospheric Sciences*, *72*(1), 5–34. https://doi.org/10.1175/JAS-D-14-0004.1

Kwok, R. (2000). Recent changes in Arctic Ocean sea ice motion associated with the North Atlantic Oscillation. *Geophysical Research Letters*, *27*(6), 775–778. https://doi.org/10.1029/1999GL002382

Lejeune, Q., Davin, E. L., Guillod, B. P., & Seneviratne, S. I. (2015). Influence of Amazonian deforestation on the future evolution of regional surface fluxes, circulation, surface temperature and precipitation. *Climate Dynamics*, *44*(9–10), 2769–2786. https://doi.org/10.1007/S00382-014-2203-8

Lenton, T. M., Held, H., Kriegler, E., Hall, J. W., Lucht, W., Rahmstorf, S., & Schellnhuber, H. J. (2008). Tipping elements in the Earth's climate system. *Proceedings of the National Academy of Sciences of the United States of America*, *105*(6), 1786–1793. https://doi.org/10.1073/pnas.0705414105

Li, C., Lu, R., & Chen, G. (2017). Promising prediction of the monsoon trough and its implication for tropical cyclone activity over the western North Pacific. *Environmental Research Letters*, *12*(7). https://doi.org/10.1088/1748-9326/aa71bd

Lwin, T. (2000). *The Prevailing Synoptic Situations in Myanmar.*

Mantua, N. J., & Hare, S. R. (2002). The Pacific Decadal Oscillation. *Journal of Oceanography*, *58*(1), 35–44. https://doi.org/10.1023/A:1015820616384

Maslanik, J. A., Serreze, M. C., & Barry, R. G. (1996). Recent decreases in Arctic summer ice cover and linkages to atmospheric circulation anomalies. *Geophysical Research Letters*, *23*(13), 1677–1680. https://doi.org/10.1029/96GL01426

Min, S. K., Zhang, X., Zwiers, F. W., & Agnew, T. (2008). Human influence on Arctic sea ice detectable from early 1990s onwards. *Geophysical Research Letters*, *35*(21). https://doi.org/10.1029/2008GL035725

Moore, G. W. K., & Pickart, R. S. (2012). The Wrangel Island Polynya in early summer: Trends and relationships to other polynyas and the Beaufort Sea High. *Geophysical Research Letters*, *39*(5). https://doi.org/10.1029/2011GL050691

Mueller, B. L., Gillett, N. P., Monahan, A. H., & Zwiers, F. W. (2018). Attribution of Arctic sea ice decline from 1953 to 2012 to influences from natural, greenhouse gas, and

https://doi.org/10.5194/egusphere-2025-521
Preprint. Discussion started: 18 February 2025


anthropogenic aerosol forcing. *Journal of Climate*, *31*(19), 7771–7787. https://doi.org/10.1175/JCLI-D-17-0552.1

Nigam, S., & Baxter, S. (2015a). General Circulation of the Atmosphere: Teleconnections. *Encyclopedia of Atmospheric Sciences: Second Edition*, 90–109. https://doi.org/10.1016/B978-0-12-382225-3.00400-X

Nigam, S., & Baxter, S. (2015b). General Circulation of the Atmosphere: Teleconnections. *Encyclopedia of Atmospheric Sciences: Second Edition*, 90–109. https://doi.org/10.1016/B978-0-12-382225-3.00400-X

Notz, D., & Marotzke, J. (2012). Observations reveal external driver for Arctic sea-ice retreat. *Geophysical Research Letters*, *39*(8). https://doi.org/10.1029/2012GL051094

Oo, K. T. (2022). Interannual Variability of Winter Rainfall in Upper Myanmar. *Journal of Sustainability and Environmental Management*, *1*(3), 344–358. https://doi.org/https://doi.org/10.3126/josem.v1i3.48001

Oo, K. T. (2023). Climatology Definition of the Myanmar Southwest Monsoon (MSwM): Change Point Index (CPI). *Advances in Meteorology*, *2023*, 2346975. https://doi.org/10.1155/2023/2346975

Oo, K. T., Dong, Y., & Jonah, K. (2025). The variability and predictability of summer southwest monsoon intensity measurement index across mainland indochina: from local synoptic to large scale perspectives. *Environmental Research Communications*, *7*(1), 15038. https://doi.org/10.1088/2515-7620/ad8107

Oo, K. T., Dong, Y., & JONAH, K. (2024). The variability and predictability of Summer Southwest Monsoon Intensity measurement index across Mainland Indochina: From Local synoptic to Large Scale Perspectives. *Environmental Research Communications*. https://doi.org/10.1088/2515-7620/AD8107

Overland, J. E. (2021). Rare events in the Arctic. *Climatic Change*, *168*(3–4). https://doi.org/10.1007/S10584-021-03238-2

Parkinson, C. L., Cavalieri, D. J., Gloersen, P., Zwally, H. J., & Comiso, J. C. (1999). Arctic sea ice extents, areas, and trends, 1978-1996. *Journal of Geophysical Research: Oceans*, *104*(C9), 20837–20856. https://doi.org/10.1029/1999JC900082

Patil, S. D., Singh, H. N., Bansod, S. D., & Singh, N. (2011). Trends in extreme mean sea level pressure and their characteristics during the summer monsoon season over the Indian region. *Https://Doi.Org/10.1080/01431161.2010.517793*, *32*(3), 701–715. https://doi.org/10.1080/01431161.2010.517793

Perovich, D. K., & Richter-Menge, J. A. (2009). Loss of sea ice in the arctic. *Annual Review*

https://doi.org/10.5194/egusphere-2025-521
Preprint. Discussion started: 18 February 2025


*of Marine Science*, *1*, 417–441. https://doi.org/10.1146/ANNUREV.MARINE.010908.163805

Pinto, J. G., & Raible, C. C. (2012). Past and recent changes in the North Atlantic oscillation. *Wiley Interdisciplinary Reviews: Climate Change*, *3*(1), 79–90. https://doi.org/10.1002/WCC.150

Qu, B., Gabric, A. J., Zhu, J. N., Lin, D. R., Qian, F., & Zhao, M. (2012). Correlation between sea surface temperature and wind speed in Greenland Sea and their relationships with NAO variability. *Water Science and Engineering*, *5*(3), 304–315. https://doi.org/10.3882/j.issn.1674-2370.2012.03.006

Reynolds, R. W., Rayner, N. A., Smith, T. M., Stokes, D. C., & Wang, W. (2002). An improved in situ and satellite SST analysis for climate. *Journal of Climate*, *15*(13), 1609–1625. https://doi.org/10.1175/1520-0442(2002)015<1609:AIISAS>2.0.CO;2

Riaz, S. M. F., Iqbal, M. J., & Adeel, M. (2021). Role of sea-level pressure of Arabian Sea on variability of summer monsoon rainfall over Northern Pakistan. *Theoretical and Applied Climatology*, *145*(1), 861–874. https://doi.org/10.1007/s00704-021-03668-z

Rodwell, M. J., & Hoskins, B. J. (1996). Monsoons and the dynamics of deserts. *Quarterly Journal of the Royal Meteorological Society*, *122*(534), 1385–1404. https://doi.org/10.1002/QJ.49712253408

Satyanarayana, G. C., Dodla, V. B. R., & Srinivas, D. (2020). Decreasing southwest monsoon rainfall over Myanmar in the prevailing global warming era. *Meteorological Applications*, *27*(1), 1–13. https://doi.org/10.1002/met.1816

Sein, K. K., Chidthaisong, A., & Oo, K. L. (2018). Observed Trends and Changes in Temperature and Precipitation Extreme Indices over Myanmar. *Atmosphere 2018, Vol. 9, Page 477*, *9*(12), 477. https://doi.org/10.3390/ATMOS9120477

Sein, Z. M. M., Ogwang, B., Ongoma, V., Ogou, F. K., & Batebana, K. (2015). Inter-annual variability of May-October rainfall over Myanmar in relation to IOD and ENSO. *Journal of Environmental and Agricultural Sciences*, *4*, 28–36.

Serreze, M. C., & Barrett, A. P. (2011). Characteristics of the Beaufort Sea high. *Journal of Climate*, *24*(1), 159–182. https://doi.org/10.1175/2010JCLI3636.1

Shaw, T. A. (2014). On the role of planetary-scale waves in the abrupt seasonal transition of the Northern Hemisphere general circulation. *Journal of the Atmospheric Sciences*, *71*(5), 1724–1746. https://doi.org/10.1175/JAS-D-13-0137.1

Spall, M. A. (2019). Dynamics and thermodynamics of the mean transpolar drift and ice thickness in the Arctic Ocean. *Journal of Climate*, *32*(24), 8449–8463.

https://doi.org/10.5194/egusphere-2025-521
Preprint. Discussion started: 18 February 2025


https://doi.org/10.1175/JCLI-D-19-0252.1

Stroeve, J. C., Kattsov, V., Barrett, A., Serreze, M., Pavlova, T., Holland, M., & Meier, W. N. (2012). Trends in Arctic sea ice extent from CMIP5, CMIP3 and observations. *Geophysical Research Letters*, *39*(16). https://doi.org/10.1029/2012GL052676

Stroeve, J., Serreze, M., Drobot, S., Gearheard, S., Holland, M., Maslanik, J., Meier, W., & Scambos, T. (2008). Arctic sea ice extent plummets in 2007. *Eos*, *89*(2), 13–14. https://doi.org/10.1029/2008EO020001

Sundaram, S., & Holland, D. M. (2022). A Physical Mechanism for the Indian Summer Monsoon—Arctic Sea-Ice Teleconnection. *Atmosphere*, *13*(4), 566. https://doi.org/10.3390/ATMOS13040566/S1

Swart, N. (2017). Climate variability: Natural causes of Arctic sea-ice loss. *Nature Climate Change*, *7*(4), 239–241. https://doi.org/10.1038/NCLIMATE3254

Thwe, H. M., Kristiansen, P., & Herridge, D. F. (2019). Benchmarks for improved productivity and profitability of monsoon rice in lower Myanmar. *Field Crops Research*, *233*, 59–69. https://doi.org/10.1016/J.FCR.2019.01.004

Timmermans, M. L., & Marshall, J. (2020). Understanding Arctic Ocean Circulation: A Review of Ocean Dynamics in a Changing Climate. *Journal of Geophysical Research: Oceans*, *125*(4). https://doi.org/10.1029/2018JC014378

Trenberth, K. E., Branstator, G. W., Karoly, D., Kumar, A., Lau, N. C., & Ropelewski, C. (1998). Progress during TOGA in understanding and modeling global teleconnections associated with tropical sea surface temperatures. *Journal of Geophysical Research: Oceans*, *103*(C7), 14291–14324. https://doi.org/10.1029/97JC01444

Vernekar, A. D., Zhou, J., & Shukla, J. (1995). The Effect of Eurasian Snow Cover on the Indian Monsoon. *Journal of Climate*, *8*(2), 248–266. https://doi.org/https://doi.org/10.1175/1520-0442(1995)008<0248:TEOESC>2.0.CO;2

Vihma, T. (2014). Effects of Arctic Sea Ice Decline on Weather and Climate: A Review. *Surveys in Geophysics*, *35*(5), 1175–1214. https://doi.org/10.1007/S10712-014-9284-0

Walsh, J. E., Fetterer, F., Scott Stewart, J., & Chapman, W. L. (2017). A database for depicting Arctic sea ice variations back to 1850. *Geographical Review*, *107*(1), 89–107. https://doi.org/10.1111/J.1931-0846.2016.12195.X

Wang, B., Ding, Q., Fu, X., Kang, I. S., Jin, K., Shukla, J., & Doblas-Reyes, F. (2005). Fundamental challenge in simulation and prediction of summer monsoon rainfall. *Geophys Res Lett*, *32*(15), L15711. https://doi.org/10.1029/2005gl022734

Wang, B., & Fan, Z. (1999). Choice of South Asian Summer Monsoon Indices. *Bulletin of the*

https://doi.org/10.5194/egusphere-2025-521
Preprint. Discussion started: 18 February 2025


*American Meteorological Society*, *80*(4), 629–638. https://doi.org/10.1175/1520-0477(1999)080<0629:COSASM>2.0.CO;2

Wang, B., & Ho, L. (2002). Rainy season of the Asian-Pacific summer monsson. *Journal of Climate*, *15*(4), 386–398. https://doi.org/10.1175/1520-0442(2002)015<0386:RSOTAP>2.0.CO;2

Wang, C. (2002). Atlantic Climate Variability and Its Associated Atmospheric Circulation Cells. *Journal of Climate*, *15*(13), 1516–1536. https://doi.org/10.1175/1520-0442(2002)015

Wang, L., & Chen, W. (2014). The East Asian winter monsoon: Re-amplification in the mid-2000s. *Chinese Science Bulletin*, *59*(4), 430–436. https://doi.org/10.1007/S11434-013-0029-0

Webb, E. J., & Magi, B. I. (2022). The Ensemble Oceanic Niño Index. *International Journal of Climatology*. https://doi.org/10.1002/JOC.7535

Webster, P. (2020). Dynamics of The Tropical Atmosphere and Oceans. *Dynamics of The Tropical Atmosphere and Oceans*. https://doi.org/10.1002/9781118648469

Webster, P. J. (1983). Mechanisms of Monsoon Low-Frequency Variability: Surface Hydrological Effects. *Journal of the Atmospheric Sciences*, *40*(9), 2110–2124. https://doi.org/10.1175/1520-0469(1983)040

Webster, P. J., & Yang, S. (1992). Monsoon and Enso: Selectively Interactive Systems. *Quarterly Journal of the Royal Meteorological Society*, *118*(507), 877–926. https://doi.org/10.1002/qj.49711850705

Xue, F., & He, J. X. (2007). The influence of the extratropical atmospheric disturbances on ENSO. *Acta Geophysica Sinica*, *50*(5), 1311–1318. https://doi.org/10.1002/CJG2.1132

Yadav, R. K. (2009). Changes in the large-scale features associated with the Indian summer monsoon in the recent decades. *International Journal of Climatology*, *29*(1), 117–133. https://doi.org/10.1002/JOC.1698

Yadav, R. K., Rupa Kumar, K., & Rajeevan, M. (2009). Increasing influence of ENSO and decreasing influence of AO/NAO in the recent decades over northwest India winter precipitation. *Journal of Geophysical Research: Atmospheres*, *114*(D12). https://doi.org/10.1029/2008JD011318

Yatagai, A., Kamiguchi, K., Arakawa, O., Hamada, A., Yasutomi, N., & Kitoh, A. (2012). Aphrodite constructing a long-term daily gridded precipitation dataset for Asia based on a dense network of rain gauges. *Bulletin of the American Meteorological Society*, *93*(9), 1401–1415. https://doi.org/10.1175/BAMS-D-11-00122.1

https://doi.org/10.5194/egusphere-2025-521
Preprint. Discussion started: 18 February 2025


Yin, M. T. (1949). SYNOPTIC-AEROLOGIC STUDY OF THE ONSET OF THE SUMMER MONSOON OVER INDIA AND BURMA. *Journal of Meteorology*, *6*(6), 393–400. https://doi.org/10.1175/1520-0469(1949)006<0393:SASOTO>2.0.CO;2

Zaw, Z., Fan, Z. X., Bräuning, A., Xu, C. X., Liu, W. J., Gaire, N. P., Panthi, S., & Than, K. Z. (2020). Drought Reconstruction Over the Past Two Centuries in Southern Myanmar Using Teak Tree-Rings: Linkages to the Pacific and Indian Oceans. *Geophysical Research Letters*, *47*(10). https://doi.org/10.1029/2020GL087627

Zin Mie Mie Sein, B. Ogwang, V. Ongoma, Faustin Katchele Ogou, & Kpaikpai Batebana. (2015). *Inter-annual variability of Summer Monsoon Rainfall over Myanmar in relation to IOD and ENSO* (pp. 4:28-36). Journal of Environmental and Agricultural Sciences.